

Scaling of Excitations across the Phases of the Kitaev Honeycomb Model

Benoît Fanton,^{1,2} under the supervision of Marin Bukov,² Patrick M. Lenggenhager,² Michael Kolodrubetz,³ and Tarik Yefsah^{1,4}

¹*École Normale supérieure-PSL*

²*Max Planck Institute for the Physics of Complex Systems*

³*University of Texas at Dallas*

⁴*Laboratoire Kastler Brossel*

(Dated: February-June 2024)

A possible way to construct a stable quantum computer could be to engineer topologically protected states that are by definition unaltered by small perturbations. One such possible state could be anyons which are particles with an exchange statistic different from the fermions and the bosons. However, we first need to create them in a lab in order to study them. As they are excitations, they can not exist in a ground state but could be obtained after out-of-equilibrium dynamics. The goal of my internship was to study the Kitaev Honeycomb model which exhibits such anyonic behavior, and use the Kibble-Zurek mechanism to understand which states are excited after a ramp in the parameters.

This report presents some studies I did during my spring internship for the validation of my M1. I did this internship at the Max Planck Institute for the Physics of Complex Systems (MPI-PKS) in Dresden under the supervision of Marin Bukov and Patrick Lenggenhager. I was also in collaboration with Michael Kolodrubetz from UT Dallas and Tarik Yefsah from the LKB.

I studied the excitations we get from non-equilibrium dynamics in the Kitaev Honeycomb model. The first two months were focused on understanding the different useful themes: the Kibble-Zurek mechanism, the band topology in condensed matter, and the Kitaev Honeycomb model. Then, I did more personal work to understand the excitations that are created after a ramp in the Kitaev model. This was done in different conditions in particular with periodic boundary conditions both analytically and numerically, and with open boundary conditions, numerically. At the end of my internship, I was also given the chance to present my work in the internal seminar of condensed matter at MPI-PKS and in the poster sessions of the workshop "Non-equilibrium Many-body Physics Beyond the Floquet Paradigm" at PKS.

In this report, I will be interested in presenting the excitations we get after a ramp of a coupling parameter in the Kitaev Honeycomb model. We will be, first, focused on the Kibble-Zurek mechanism which studies what happens when we are crossing dynamically a second-order phase transition, which here will be quantum; I will in particular explain it in the case of the transverse field Ising model. Then I will present, the Kitaev Honeycomb model and how it could be extended

to have a chiral phase. Finally, I will combine the two and study the Kibble-Zurek mechanism in the Kitaev model with different conditions.

CONTENTS

I. Kibble-Zurek Mechanisms	2
A. Landau-Zener transition	2
B. Transverse field Ising model	3
C. Out of equilibrium dynamics	4
D. General mechanism	5
II. Solving the model	6
A. Original model	6
B. Phase diagram	7
C. Extended version	8
III. Out of equilibrium dynamics for the Honeycomb model	9
A. Periodic boundary condition on the Kitaev model	9
B. Periodic boundary condition on the extended model	12
C. Excitation of the edge modes in the extended model	14
Conclusion	15
References	15
A. Computation of the log-correction	15
B. Circumstances of log-correction	17

I. KIBBLE-ZUREK MECHANISMS

A. Landau-Zener transition

In order to understand well the mechanism let's first focus on the simple case of a Landau-Zener transition — which will also be a building block for the other situations. We consider a two-level system (for instance a $\frac{1}{2}$ -spin particle) where we have a time evolution such that the ground state becomes the excited state (and reversely). During this exchange, as we are in quantum mechanics, we may suppose that there is also a hybridization between the two states. A simple Hamiltonian which represents this phenomenon can be :

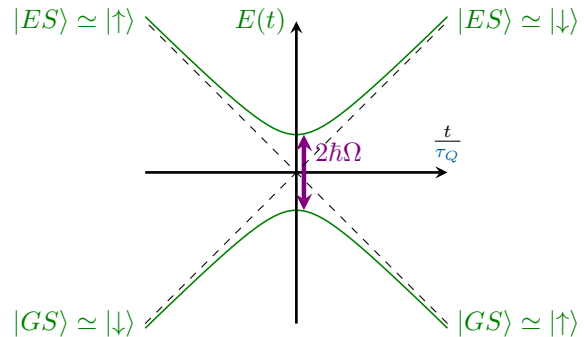
$$H = \begin{pmatrix} -\varepsilon \frac{t}{\tau_Q} & \hbar\Omega \\ \hbar\Omega & \varepsilon \frac{t}{\tau_Q} \end{pmatrix}. \quad (1)$$

Here, $2\varepsilon \frac{t}{\tau_Q}$ is the energy of the gap between the ground state and the excited state at infinite times ($|t| \gg \tau_Q$), it changes sign at $t = 0$ which represent the change between the two states; τ_Q is the "quench time" it is the characteristic time scale of the evolution. We also have an off-diagonal term $\hbar\Omega$ which makes the two systems hybridize, moreover, as we can see in the next graph it also represents the gap between the two states at $t = 0$. In particular, it is this term which dominates at low times ($|t| \ll \tau_Q$).

We can diagonalize this Hamiltonian, it has the two eigenvalues $\pm E(t) = \pm \sqrt{\left(\varepsilon \frac{t}{\tau_Q}\right)^2 + (\hbar\Omega)^2}$, and the corresponding eigenstates are :

$$\begin{cases} |ES\rangle \propto \begin{pmatrix} \varepsilon \frac{t}{\tau_Q} - E \\ -\hbar\Omega \end{pmatrix} \\ |GS\rangle \propto \begin{pmatrix} \varepsilon \frac{t}{\tau_Q} + E \\ -\hbar\Omega \end{pmatrix} \end{cases}. \quad (2)$$

In particular, if we note: $|\downarrow\rangle = \begin{pmatrix} 1 \\ 0 \end{pmatrix}$ and $|\uparrow\rangle = \begin{pmatrix} 0 \\ 1 \end{pmatrix}$, we have the exchange between the ground state and the excited states as in the following schematics :



This was the study of the instantaneous eigenstates but what we are interested in, is the time evolution of an initial state after a Schrödinger evolution :

$$i\hbar \frac{\partial |\psi\rangle}{\partial t} = H |\psi\rangle. \quad (3)$$

We suppose that we start at a time $t_0 < 0$ such that $|t_0| \gg \tau_Q$ i.e. we are in the limit $t \rightarrow -\infty$. We begin the evolution in the ground state $\psi(t_0) = |\downarrow\rangle$. Then, we can write in general $\psi(t) = \alpha(t) |GS(t)\rangle + \beta(t) |ES(t)\rangle$. If we do a measure at time t , we will have a probability $p(t) = |\beta(t)|^2$ to be excited and for instance $p(t_0) = 0$. A very useful tool to continue our study is the adiabatic theorem first presented by Born and Fock in [1]. This theorem states that for an evolution slow compared to the gap between the states (or more precisely to the inverse of the gap divided by \hbar) then there is no transition between different states. This implies in our study that for infinite times as the gap is very large there is no transition. In other word for $t_1 < 0$ and $|t_1| \gg \tau_Q$, we have $p(t_1) \simeq p(t_0) = 0$ and for $t_2 > t_3 \gg \tau_Q$, $p(t_2) \simeq p(t_3)$. This enables to have a good definition of the Landau-Zener transition which is $p_{LZ} = p(t_2)$ (with $t_2 \gg \tau_Q$), this quantity does not depend on t_0 nor on t_2 . It is the probability to be excited at infinite time

There can be different ways to compute this value p_{LZ} , but I will not develop them here. We can find it for instance in the original paper by Zener in [2]. We get :

$$p_{LZ} = \exp\left(-\frac{\pi(\hbar\Omega)^2}{\varepsilon \frac{\hbar}{\tau_Q}}\right). \quad (4)$$

From here, to simplify notation, we will take units such that $\varepsilon = 1$, which gives an energy scale, and such that $\hbar = 1$, this unites the notion of time and energy in quantum mechanics. This gives us a new expression for the Landau-Zener transition :

$$p_{LZ} = \exp(-\pi\Omega^2\tau_Q). \quad (5)$$

This means that there will be no excitation for $\Omega \gg \frac{1}{\sqrt{\tau_Q}}$. It is exactly the adiabatic theorem: for a large gap or slow evolution we have no transition from the ground state to the excited state. Here we have something more specific because it also gives us the scale; which could have also been found by dimension analysis if we did not have taken dimensionless variables.

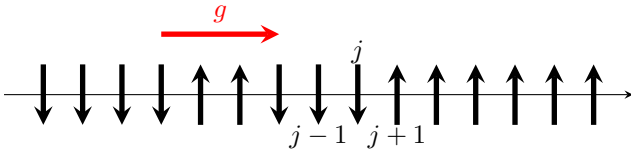
This is what we will use next, when we have an evolution of characteristic time τ_Q and minimal energy Ω , there can be excitation from the ground state to the excited state iff :

$$\Omega \lesssim \frac{1}{\sqrt{\tau_Q}}. \quad (6)$$

Now that we have understood this building block we can now go to a more complex system: the transverse field Ising model.

B. Transverse field Ising model

In order to understand the Kibble-Zurek mechanism we will first present it for a solvable model, the Transverse Field Ising Model (TFIM). This subsection and the next one are in particular based on the work of Dziarmaga in [3]. The system that we consider is a chain of $\frac{1}{2}$ -spins coupled by an Ising term according to the z direction. In addition to that, we suppose that there is a transverse magnetic field g in the x direction.



This leaves us the Hamiltonian :

$$H = - \sum_j g \sigma_j^x + \sigma_j^z \sigma_{j+1}^z. \quad (7)$$

As a reminder, we take dimensionless factors such that $\hbar = 1$ and the energy of the Ising coupling is 2. In the thermodynamic limit i.e. for a large value N of the number of spins, this system exhibits a phase transition. This can be already seen by the fact that for large value of the field $g \gg 1$, the ground state will be the unique state where all the spins are aligned with the field $|\rightarrow \rightarrow \rightarrow \dots\rangle$, it is paramagnetic; whereas for vanishing field $g = 0$, we have two degenerate ground states $|\uparrow \uparrow \uparrow \dots\rangle$ and $|\downarrow \downarrow \downarrow \dots\rangle$, it is ferromagnetic. These two situations represent two phases and therefore there will be a point where we have a phase transition. We

will see that, here, it happens for $g = 1$.

First, to solve our model, we make a change of variable called the Jordan Wigner transformation such that, instead of having a chain of spins, we consider having a chain of positions, where a fermion could or could not be. We note c_j the operator annihilation of the fermion on the point j and we consider the change :

$$\begin{cases} \sigma_j^x = 1 - 2c_j^\dagger c_j \\ \sigma_j^z = -(c_j^\dagger + c_j) \prod_{j' < j} \sigma_{j'}^x \end{cases} \quad (8)$$

With this, we get a Hamiltonian

$$H = - \sum_j \frac{g}{2} - g c_j^\dagger c_j + c_j^\dagger c_{j+1} + c_{j+1} c_j + H.c.. \quad (9)$$

We go in the thermodynamic limit where N the number of spins is large compared to 1, the boundary limit does not change anything so we can consider that it is periodic: $c_{N+1} = c_1$. We can then do a Fourier transform

$$c_j = \frac{1}{\sqrt{N}} \sum_k c_k e^{ikj} \quad (10)$$

where k takes value in $\{0, \frac{2\pi}{N}, \dots, \frac{2\pi(N-1)}{N}\}$. This gives us the new Hamiltonian :

$$H = -2 \sum_k \begin{pmatrix} c_k^\dagger & c_{-k} \end{pmatrix} \begin{pmatrix} g - \cos(k) & \sin(k) \\ \sin(k) & -(g - \cos(k)) \end{pmatrix} \begin{pmatrix} c_k \\ c_{-k}^\dagger \end{pmatrix}. \quad (11)$$

This can be interpreted as fermions for each quasi momentum k which interact only with themselves and the $-k$ fermion. We can finally do a Bogoliubov-De Gennes transformation where we mix the k and $-k$. This can be done by the diagonalization of the matrix :

$$H_k = 2 \begin{pmatrix} g - \cos(k) & \sin(k) \\ \sin(k) & -(g - \cos(k)) \end{pmatrix} \quad (12)$$

which has the eigenvalues $\pm \varepsilon_k = \pm \sqrt{(g - \cos(k))^2 + \sin^2(k)}$ and the associated eigenvectors $\begin{pmatrix} u_k^\pm \\ v_k^\pm \end{pmatrix}$. Then we define the annihilation operator

$$\gamma_k = u_k^\dagger c_k + v_k^\dagger c_{-k}^\dagger \quad (13)$$

and with this, the Hamiltonian becomes :

$$H = \sum_k \varepsilon \left(\gamma_k^\dagger \gamma_k - \frac{1}{2} \right). \quad (14)$$

It means that the fermions γ_k represent the excitations of the system: the ground state is achieved with the vacuum of the γ_k and each presence of a fermion is an additional energy ε_k . These γ_k will be our main interest because they simply represent the system. The excitation energies ε_k vanish only for $k = 0$ and $g = 1$ (for $g \geq 0$). It means that the ground state is gaped for $g \neq 1$; therefore, the point of the phase transition between ferromagnetic and paramagnetic phases is at $g = 1$.

C. Out of equilibrium dynamics

We now consider what happens if we change the tuning parameter $g(t)$ with time. We will start from the ground state. For a simple resolution, we take $g(t) = 1 - \frac{t}{\tau_Q}$ with t going from $-\infty$ to τ_Q such that a phase transition happened at $t = 0$. We consider slow evolution (τ_Q large) therefore by the adiabatic theorem, we have excitation only for vanishing energy. However, inside a phase, there is a gap and no vanishing energy so excitations happen only at the phase transition; we will see that in detail afterward. We get a Hamiltonian $H = \sum_k \varepsilon_{g(t),k} \left(\gamma_{g(t),k}^\dagger \gamma_{g(t),k} - \frac{1}{2} \right)$ where all the different terms vary with time. As we are not in an equilibrium situation, the probability of having an excitation varies with time, it is $p_k(t) = \langle \gamma_{g(t),k}^\dagger \gamma_{g(t),k} \rangle_t$. The core of our study will be the study of the number of excitations :

$$\mathcal{N} = \sum_k \langle \gamma_{g(t),k}^\dagger \gamma_{g(t),k} \rangle_t = \sum_k p_k. \quad (15)$$

With a system of size N we can consider more precisely the density of excitations which is size invariant in the large N limit :

$$\nu = \frac{\mathcal{N}}{N} \simeq \int_{BZ} \frac{dk}{2\pi} p_k \quad (16)$$

Therefore, we want to get an expression (or at least an approximation) of p_k . For that, we can take the Heisenberg picture which gives the expression (with ψ_i the initial vector) :

$$\langle \gamma_{g(t),k}^\dagger \gamma_{g(t),k} \rangle_t = \langle \psi_i | \gamma_{g,k,t}^\dagger \gamma_{g,k,t} | \psi_i \rangle = \left| \gamma_{g,k,t} | \psi_i \rangle \right|^2. \quad (17)$$

By taking, the Heisenberg picture in (13), we have :

$$\gamma_{g,k,t} = u_{g,k} c_{k,t} + v_{g,k} c_{-k,t}^\dagger = (u_{g,k} \ v_{g,k}) \begin{pmatrix} c_{k,t} \\ c_{-k,t}^\dagger \end{pmatrix} \quad (18)$$

where all the dependencies are explicit and we write $u = u^+$ and $v = v^+$. Now we can use the Heisenberg equation :

$$i\partial_t \begin{pmatrix} c_{k,t} \\ c_{-k,t}^\dagger \end{pmatrix} = \left[\begin{pmatrix} c_{k,t} \\ c_{-k,t}^\dagger \end{pmatrix}, H(t) \right] = H_k(t) \begin{pmatrix} c_{k,t} \\ c_{-k,t}^\dagger \end{pmatrix}. \quad (19)$$

Therefore, with $U_k(t)$ the evolution operator of H_k as an Hamiltonian, we have :

$$\begin{pmatrix} c_{k,t} \\ c_{-k,t}^\dagger \end{pmatrix} = U_k(t) \begin{pmatrix} c_{k,t_i} \\ c_{-k,t_i}^\dagger \end{pmatrix}. \quad (20)$$

This gives us :

$$p_k(t) = |\gamma_{g,k,t} | \psi_i \rangle|^2 = \left| (u_{g,k} \ v_{g,k}) U_k(t) \begin{pmatrix} c_{k,t_i} \\ c_{-k,t_i}^\dagger \end{pmatrix} | \psi_i \rangle \right|^2. \quad (21)$$

However, by inverting (13) we also have :

$$\begin{pmatrix} c_{k,t_i} \\ c_{-k,t_i}^\dagger \end{pmatrix} = \begin{pmatrix} u_{k,g_i} & -v_{k,g_i} \\ v_{k,g_i} & u_{k,g_i} \end{pmatrix} \begin{pmatrix} \gamma_{g_i,k,t_i} \\ \gamma_{g_i,-k,t_i}^\dagger \end{pmatrix} \quad (22)$$

and we finally get :

$$p_k(t) = \left| (u_{g,k} \ -v_{g,k}) U_k(t) \begin{pmatrix} u_{k,g_i} & -v_{k,g_i} \\ v_{k,g_i} & u_{k,g_i} \end{pmatrix} \begin{pmatrix} \gamma_{g_i,k,t_i} \\ \gamma_{g_i,-k,t_i}^\dagger \end{pmatrix} | \psi_i \rangle \right|^2. \quad (23)$$

We started from the ground state i.e. it is the vacuum of the fermion γ_{g_i,k,t_i} and therefore :

$$\begin{cases} |\gamma_{g_i,k,t_i} | \psi_i \rangle|^2 = 0 \\ |\gamma_{g_i,-k,t_i}^\dagger | \psi_i \rangle|^2 = 1 \end{cases} \quad (24)$$

for all k . This simplifies (23) which becomes

$$p_k(t) = \left| (u_{g,k} \ v_{g,k}) U_k(t) \begin{pmatrix} -v_{k,g_i} \\ u_{k,g_i} \end{pmatrix} \right|^2 \quad (25)$$

and this is easy to understand physically, it is the probability of being in the excited state of $H_k(t)$ after an evolution ruled by $H_k(t)$ and starting from the ground state of $H_k(t_i)$. But we can spot that $H_k(t)$ is a Landau-Zener evolution

$$H_k(t) = 2 \begin{pmatrix} -\frac{\tau_k}{\tau_Q} & \Omega_k \\ \Omega_k & \frac{\tau_k}{\tau_Q} \end{pmatrix} \quad (26)$$

with $\tau_k = t - \tau_Q(1 - \cos(k))$ and $\Omega_k = \sin(k)$. This gives us $p_k(t)$ as the Landau-Zener transition at τ_k . We end the evolution at $t_f = \tau_Q$, therefore we have $\tau_{k,f} > 0$ for $-\frac{\pi}{2} < k < \frac{\pi}{2}$. We suppose that we have slow evolution, meaning that $\tau_Q \gg 1$ and the Landau-Zener

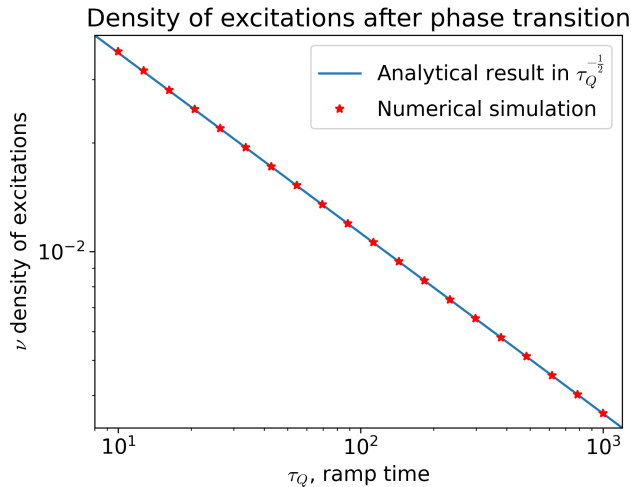


FIG. 1: Density of excitation after a ramp in the transverse field Ising model for a large system. In the infinite τ_Q limit we have excitations which scale as $\tau_Q^{-\frac{1}{2}}$ and here we also have an explicit solution.

transition is quantitative only if $\Omega_k = \sin(k) \lesssim \tau_Q^{-\frac{1}{2}} \ll 1$ i.e. $k \ll 1$. In particular for these values, $\Omega_k \ll \tau_{k,f}$ and we are well within the infinite time limit. As these are the only quantitative excitations, we can make the approximation :

$$p_k(t) = \exp(-2\pi\Omega_k^2\tau_Q) \simeq \exp(-2\pi k^2\tau_Q) \quad (27)$$

with the 2 coming from the prefactor in H_k . Finally, we can compute exactly the density of excitations :

$$\nu = \frac{1}{2\pi} \int_{-\pi}^{\pi} dk p_k(t) \simeq \frac{1}{2\pi} \int_{-\infty}^{\infty} \exp(-2\pi k^2\tau_Q) \quad (28)$$

$$\nu = \frac{1}{\pi\sqrt{2\tau_Q}}. \quad (29)$$

We have an exact solution of the density of excitation, in particular, we have the scaling of the excitations as $\tau_Q^{-\frac{1}{2}}$ which we can get generically from the universality classes as presented in the next subsection. This was the theoretical approach but it can also be observed numerically, by computing the different p_k and adding them. We get the results in FIG. 1. They agree very well with what we expected.

Here we can spot that in our study the excitations happen for $k \simeq 0$ and therefore around $t_f \simeq 0$. This comes from the adiabatic theorem, we have no excitation if the energy is $\gtrsim \tau_Q^{-\frac{1}{2}}$, therefore for large τ_Q , there

is no excitation in the gapped phases, everything happens at the phase transition and if we stopped the evolution at $t = -\frac{\tau_Q}{2}$ or $\frac{\tau_Q}{2}$ it would not change the density of excitations.

D. General mechanism

We have seen what happens to the density of excitations when we cross the phase transition in the TFIM, but we can get more general results with the Kibble-Zurek mechanism. This was first presented by Kibble to study cosmological phase transition after the Big Bang in [4] and extended by Zurek for generic second-order phase transitions in [5]. Here we will study more precisely how it can be interpreted for quantum phase transition at $T = 0$. The first idea of this mechanism is the fact that for slow evolution there is no excitation in a gapped phase (we follow an adiabatic evolution), therefore all the physics happens at the phase transition where the gap vanishes. But, we also have at the phase transition some universality properties so the scalings will only depend on this universality.

Let's consider a generic phase transition from a gapped phase to a gapped phase going gapless at the critical point (meaning it is second order). We name λ the tuning parameter such that the phase transition happens at $\lambda = 0$. Therefore, we have, by definition of the critical exponents, for $|\lambda| \ll 1$:

$$\begin{cases} \lambda^{-\nu} \sim \xi \propto k^{-1} \\ \xi^z \sim \tau_r \propto \Delta^{-1} \end{cases} \quad (30)$$

with ξ the correlation length, τ_r the relaxation time, k characteristic quasi-momentum and Δ the gap. We choose an evolution for which $\lambda = \frac{t}{\tau_Q}$, therefore the adiabaticity is broken when

$$\tau_r \gtrsim \left(\frac{d\Delta}{dt} \frac{1}{\Delta} \right)^{-1} \quad (31)$$

because the RHS represents the characteristic time of evolution and the LHS represents the time for the system to come back to equilibrium. We get this equality at the characteristic time :

$$t_{KZ} \sim \tau_Q^{\frac{\nu z}{1+\nu z}} \quad (32)$$

and therefore for a gap :

$$\Delta_{KZ} \sim \tau_Q^{-\frac{\nu z}{1+\nu z}}. \quad (33)$$

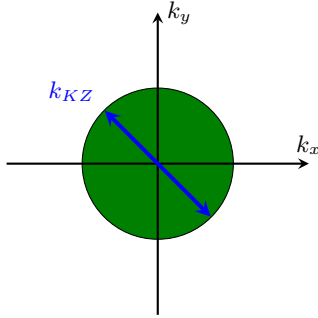


FIG. 2: Domain of the Brillouin zone where we have excitations after a ramp of characteristic time scale τ_Q .

This is the energy under which the evolution is no longer adiabatic, it is, therefore, the case for excitations represented by a quasi-momentum less than :

$$k_{KZ} \sim \tau_Q^{-\frac{\nu}{1+\nu z}}. \quad (34)$$

If we are in a system of dimension d , we finally have a domain excited as in the FIG. 2, the size of this domain scales therefore as $\tau_Q^{-\frac{d\nu}{1+\nu z}}$. If we look for the density of excitations, the scaling will be the same as the size over which excitations will appear in the Brillouin zone. Therefore, we get in general :

$$\nu \sim \tau_Q^{-\frac{d\nu}{1+\nu z}}. \quad (35)$$

This is coherent with what we had for the TFIM because in this system, $d = z = \nu = 1$ and we had $\nu \sim \tau_Q^{-\frac{1}{2}}$. These ideas are even more general, if we have the energy Δ_{KZ} , we know what is excited by just looking at the quasi-momentum for which the energy is less than Δ_{KZ} .

II. SOLVING THE MODEL

Now that we understand the Kibble-Zurek mechanism we want to apply it to a topological case but first we need to understand our model: the Kitaev-Honeycomb model. This was a model introduced by Kitaev in [6] to have a toy model which represents anyons in a solvable model. Kitaev in the same paper shows that by breaking the time-reversal symmetry the system exhibits non-commutative anyons behaviors. I did not focus my study on the anyonic behavior of the excitations but I will present how we can solve the model with and without time-reversal symmetry.

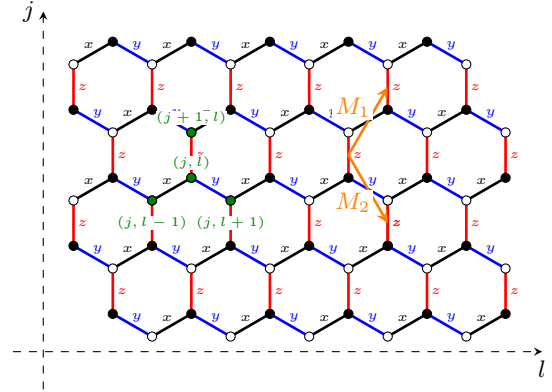


FIG. 3: Honeycomb lattice

A. Original model

We consider a system with spins $\frac{1}{2}$ on the vertices of a hexagonal lattice. We name the links x, y and z according to their orientations as in FIG. 3. We then choose the Hamiltonian :

$$H = - \sum_{x\text{-links}} J_x \sigma_n^x \sigma_m^x - \sum_{y\text{-links}} J_y \sigma_n^y \sigma_m^y - \sum_{z\text{-links}} J_z \sigma_n^z \sigma_m^z \quad (36)$$

This Hamiltonian is such that we link neighbors with different coupling and orientation depending on the nature of the link. We have in particular three coupling parameters J_x, J_y and J_z . Kitaev for his solution used a decomposition of the spins in 4 majorana fermions which enables a symmetric representation of the system. However, here I will use the Jordan Wigner transformation presented by Chen and Nussinov in [7] which is easier to implement numerically.

First, we label each site with the integers (j, l) as in FIG. 3 such that a line $j = cst$ is a horizontal line with x and y links. We can then do a Jordan-Wigner transformation saying that we have a fermion if the spin is along $+z$:

$$\begin{cases} \sigma_{jl}^z = 2c_{jl}^\dagger c_{jl} - 1 \\ \sigma_{jl}^x = (c_{jl} + c_{jl}^\dagger) \prod_{(j', l') < (j, l)} \sigma_{j'l'}^z \\ \sigma_{jl}^y = i(c_{jl}^\dagger - c_{jl}) \prod_{(j', l') < (j, l)} \sigma_{j'l'}^z \end{cases} \quad (37)$$

Here we need, to define a string of spins that are before the one we are looking at. We take the lexicographical order: $(j', l') < (j, l)$ iff $j' < j$ or if $j = j'$ and $l' < l$; in a nutshell, a spin is before another if it is below or

on the same line but before on this line. With this, the Hamiltonian becomes :

$$\begin{aligned}
H = & - \sum_{x\text{-links}} J_x (c_{jl}^\dagger + c_{jl}) (c_{jl-1}^\dagger - c_{jl-1}) \\
& - \sum_{y\text{-links}} J_y (c_{jl}^\dagger + c_{jl}) (c_{jl+1}^\dagger - c_{jl+1}) \\
& - \sum_{z\text{-links}} J_z (2c_{jl}^\dagger c_{jl} - 1) (2c_{j+1l}^\dagger c_{j+1l} - 1)
\end{aligned} \quad (38)$$

which is great because it is still local even though our Jordan-Wigner transformation is not. We can then define for each site, two Majorana fermions which define the complex fermion :

$$c_n = \frac{1}{2}(a_n + ib_n) \quad (39)$$

with $a_n^\dagger = a_n$ and $b_n^\dagger = b_n$. This transforms the Hamiltonian into :

$$H = \sum_{jl} iJ_x a_{jl} b_{jl-1} + iJ_y a_{jl} a_{jl+1} + J_z a_{jl} b_{jl} a_{j+1l} b_{j+1l} \quad (40)$$

where the sum spans only over the black sites. Here we can spot that the terms $a_{jl} = ib_{jl} a_{j+1l}$ are constants of motion (if jl represents a black site). We have $\alpha_{jl}^2 = 1$ so α_{jl} can take two eigenvalues ± 1 . We note that the α_{jl} represent the flux sector for the Majoranas a_{jl} and b_{jl+1} because for each plaquette, $\alpha_{jl} \cdot \alpha_{j+1l}$ represent the flux of the exchanges according to the Hamiltonian. According to Lieb in [8], the ground state of such a system is obtained when all the fluxes are equal to 1, therefore in this study, we place ourselves in the domain $\alpha_{jl} = 1$. This gives us the new Hamiltonian :

$$H = i \sum_{\vec{n}} J_x a_{\vec{n}} b_{\vec{n}-\vec{M}_1} + J_y a_{\vec{n}} b_{\vec{n}+\vec{M}_2} + J_z a_{\vec{n}} b_{\vec{n}} \quad (41)$$

where we consider now the sum over all vertical links z and for each link we consider $a_{\vec{n}} = a_{jl}$ and $b_{\vec{n}} = b_{j+1l}$. Now we consider a system of large size N and put the system in the periodic boundary condition. Then, we can do a Fourier transform :

$$\begin{cases} a_k = \frac{1}{\sqrt{2N}} \sum_n a_n e^{i\vec{k}\cdot\vec{n}} \\ b_k = \frac{1}{\sqrt{2N}} \sum_n b_n e^{i\vec{k}\cdot\vec{n}} \end{cases} \quad (42)$$

Implementing this in the Hamiltonian gives us :

$$H = 2 \sum_k i \left(J_x a_k b_k^\dagger e^{ik_1} + J_y a_k b_k^\dagger e^{-ik_2} + J_z a_k b_k^\dagger \right) \quad (43)$$

with $k_1 = \vec{k} \cdot \vec{M}_1$ and $k_2 = \vec{k} \cdot \vec{M}_2$. We label $\chi_k = \begin{pmatrix} a_k \\ b_k \end{pmatrix}$ where the a_k and b_k are complex fermions with $a_k^\dagger = a_{-k}$ and $b_k^\dagger = b_{-k}$, then we can write :

$$H = \sum_k \chi_k^\dagger H_k \chi_k \quad (44)$$

where the sum spans over half the Brillouin zone and

$$H_k = 2 \begin{pmatrix} 0 & i(J_z + J_x e^{-ik_1} + J_y e^{ik_2}) \\ -i(J_z + J_x e^{ik_1} + J_y e^{-ik_2}) & 0 \end{pmatrix}. \quad (45)$$

To simplify further this expression, we can label τ_x, τ_y and τ_z the Pauli matrices, and then

$$H_k = \vec{h} \cdot \vec{\tau} \quad (46)$$

with :

$$\vec{h} = 2 \begin{pmatrix} J_x \sin(k_1) - J_y \sin(k_2) \\ -(J_z + J_x \cos(k_1) + J_y \cos(k_2)) \\ 0 \end{pmatrix}. \quad (47)$$

Now we are in a situation very similar to the one of the TFIM, we can do a Bogoliubov-De Gennes transformation, with (u_k, v_k) positive eigenvector of H_k of eigenvalue ε_k :

$$\chi_k = \begin{pmatrix} u_k & -v_k^* \\ v_k & u_k^* \end{pmatrix} \begin{pmatrix} \gamma_k \\ \gamma_{-k}^\dagger \end{pmatrix} \quad (48)$$

we have

$$H = \sum_k \varepsilon_k (\gamma_k^\dagger \gamma_k - \frac{1}{2}). \quad (49)$$

Therefore we have a representation with the fermions γ_k constants of motion. The ground state is achieved for the vacuum of these fermions and each γ_k represents an excitation of energy

$$\varepsilon_k = |J_z + J_x e^{-ik_1} + J_y e^{ik_2}|. \quad (50)$$

B. Phase diagram

We have the expression of the energy of an excitation in (50). If we look at this energy as the norm of a complex number in $\mathbb{C} = \mathbb{R}^2$, it is the sum of three vectors of independent angles as in FIG. 4. In particular, ε_k can vanish if it is possible to form a triangle with the length of its sides equal to J_x, J_y and J_z , i.e. iff :

$$\begin{cases} J_x + J_y > J_z \\ J_z + J_x > J_y \\ J_y + J_z > J_x \end{cases}. \quad (51)$$

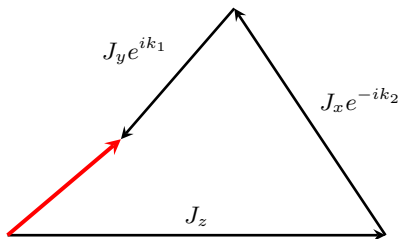


FIG. 4: Representation of ε_k in $\mathbb{C} = \mathbb{R}^2$: ε_k is the norm of the red vector.

In this situation, we are therefore in a gapless phase, otherwise, we are in a gapped phase. To represent the different possibilities we need to be able to represent the different values of J_x , J_y and J_z . To do that, we can spot that changing the sign of one J_i does not change the aspect of the spectrum up to a translation in the Brillouin zone, so we can consider $J_x, J_y, J_z > 0$. Moreover, multiplying all the J_x, J_y and J_z by the same constant λ does not change the aspect of the spectrum: it only scales it by λ . Therefore we can use the barycentric representation of three reals: we take A, B and C forming an equilateral triangle, the point (J_x, J_y, J_z) is then the point M inside the triangle such that

$$J_x \overrightarrow{MA} + J_y \overrightarrow{MB} + J_z \overrightarrow{MC} = 0 \quad (52)$$

for more information please see on Wikipedia. The important idea is that the bigger, one number is, compared to the other, the closer the point will be to a vertex of the triangle. Finally, we get the phase diagram in 5.

What we see is that we have a central gapless phase in orange and three gapped phases when one J_i is larger than the sum of the others. In [6], Kitaev showed that the gapped phases are topologically equivalent to the toric code; whereas the gapless phase exhibits anyonic behavior.

If we look more closely at the spectrum, we have different situations depending on where we are in the phase diagram.

- For the gapped phase, we won't develop more than the fact that it is gapped.
- Inside the gapless phase, we have two Dirac cones in the Brillouin zone, they exhibit linear dispersion, everywhere else in gapped.
- On the critical line (in green), we have one point of vanishing energy where there is a quadratic dispersion in one direction and a linear dispersion in the other direction. This comes from the fact that the phase transition is happening when two Dirac

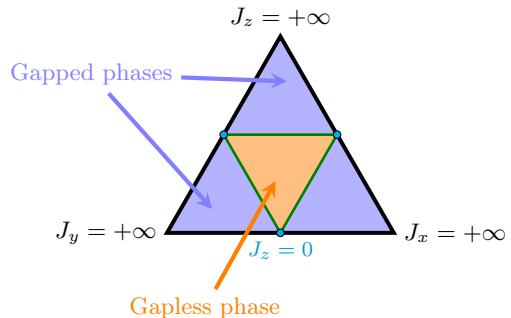


FIG. 5: Phase diagram of Kitaev honeycomb model.

cones merge, they flatten the dispersion in the direction where they meet.

- At the multicritical point (in cyan), we have an entire line in the Brillouin zone where the energy is vanishing, and the dispersion is linear in the other direction. It is because at this point we have one $J_i = 0$ and therefore the system is no longer 2D but a set of 1D lines. The $J_i = 0$ is even equivalent to the TFM and $J_x = J_y$ corresponds to the phase transition.

We can see this represented in FIG. 6.

C. Extended version

We solved the Kitaev model in the original scenario, we will now focus on the Kitaev model with a time-reversal breaking.

This was first introduced by Kitaev in [6] with a magnetic field. However, this magnetic field does not commute with the flux sector and therefore we lose the α_{jl} constants of motions; this makes our study a lot more difficult. Nevertheless, this can also be done via an effective Floquet Hamiltonian as presented by Sun and al. in [9]. This gives us a Hamiltonian :

$$H = H_K + \varepsilon \sum_{\langle\langle j,l \rangle\rangle} J_\alpha J_\gamma \sigma_j^\alpha \sigma_k^\beta \sigma_l^\gamma \quad (53)$$

with H_K the precedent Hamiltonian, the sum taken over the second-nearest neighbors and j, k, l, α, β and γ as in FIG. 7. The ε is a constant depending on the protocol we use. It must stay small to have H as a realistic Hamiltonian.

This new Hamiltonian breaks the time-reversal symmetry \mathcal{T} because $\mathcal{T} \sigma_j^\alpha = -\sigma_j^\alpha$. This will open the gap in the gapless phase because the vanishing energy was

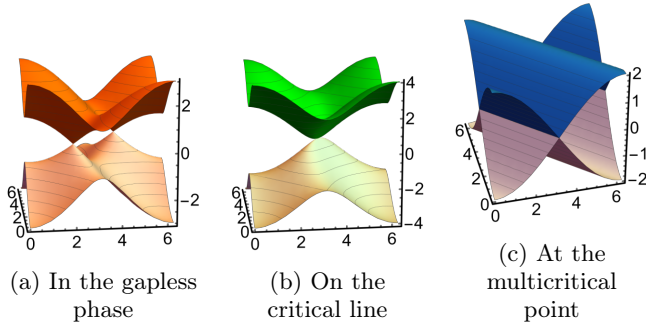


FIG. 6: Spectrum of the Kitaev model in different situations. The horizontal axes represent the Brillouin zone k and the vertical axis represents the energies $\pm\varepsilon_k$.

topologically protected by the time-reversal and the inversion symmetries (as it is the case for instance for graphene).

We can do the same transformation as in the precedent subsections, we get for instance :

$$\sigma_{j-1l}^x \sigma_{jl}^y \sigma_{jl+1}^z = i\alpha_{jl} b_{j-1l} b_{jl+1} \quad (54)$$

I will not develop all the computations but in the zero flux sector ($\alpha_{jl} = 1$), we get after Fourier transform the Hamiltonian in the form :

$$H = \sum_k \chi_k^\dagger H_k \chi_k \quad (55)$$

with $H_k = \vec{h} \cdot \vec{\tau}$ (the τ_i are the Pauli matrices) and

$$\vec{h} = 2 \begin{pmatrix} J_x \sin(k_1) - J_y \sin(k_2) \\ -(J_z + J_x \cos(k_1) + J_y \cos(k_2)) \\ 2\varepsilon(J_x J_y \sin(k_1 + k_2) - J_x J_z \sin(k_1) - J_y J_z \sin(k_2)) \end{pmatrix}. \quad (56)$$

We can also get after a Bogoliubov-De Gennes transformation :

$$H = \sum_k \varepsilon_k (\gamma_k^\dagger \gamma_k - \frac{1}{2}) \quad (57)$$

with this time :

$$\varepsilon_k = |\vec{h}| \quad (58)$$

This effectively opens the gap so we get 4 gapped phases at the same positions as in FIG. 5. On the critical green lines, we still have a phase transition, and the gap vanishes. However, this time we also have a different topology between the phases: the central orange phase

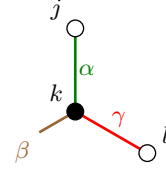


FIG. 7: Second nearest neighbors as in the Hamiltonian of the extended model.

is chiral and the extremal blue phases are topologically trivial. Kitaev showed that the excitations in this chiral phase can be seen as non-abelian anyons but I will not develop this part.

III. OUT OF EQUILIBRIUM DYNAMICS FOR THE HONEYCOMB MODEL

We have presented how to solve the equilibrium Kitaev model, now we are interested in diving into the out-of-equilibrium dynamics. In particular, we will study the density of excitation after a ramp in different situations. Some of the results of the first subsection were already done by Das and al. in [10] and Hikichi and al. in [11], but all the following work is new. The goal of my internship was in particular to study the excitations in the extended model on open boundary conditions because it enables us to understand the excitation of edge states.

A. Periodic boundary condition on the Kitaev model

We consider a ramp going through the phase diagram as in FIG. 8: we choose $J_x = J_y = 1$ and $J_z = -\frac{t}{\tau_Q}$. We start the process at $t = -\infty$ in the ground state and we will stop the process at different times. The situation is very similar to the first section, in fact, we have the same form of Hamiltonian :

$$H(t) = \sum_k \chi_k^\dagger H_k(t) \chi_k \quad (59)$$

with χ_k independent of time (in Schrödinger picture). Here we want to study

$$\nu = \frac{1}{N} \sum_k \langle \gamma_{g(t),k}^\dagger \gamma_{g(t),k} \rangle_t \quad (60)$$

and as in the first section, we have

$$\nu \simeq \int \frac{d^2k}{4\pi^2} p_k(t) \quad (61)$$

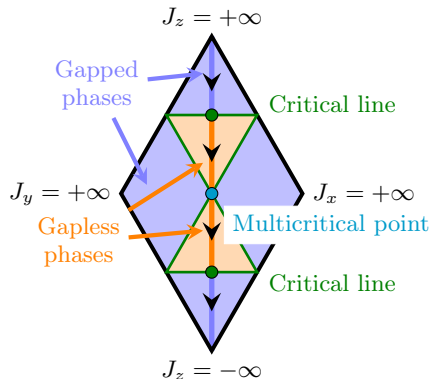


FIG. 8: Protocol of our evolution going from $J_z = +\infty$ to $J_z = -\infty$. In this representation, we also added the part of the phase diagram for negative J_z which is simply the symmetric of the upper diagram, this enables us to cross the multicritical point.

with $p_k(t)$ the probability of being in the excited state after starting in the ground state of the Hamiltonian $H_k(t)$. With a change of basis, we can even write $H_k(t)$ as the Landau-Zener Hamiltonian :

$$H_k(t) = 2 \begin{pmatrix} -\frac{\tau_k}{\tau_Q} & \Omega_k \\ \Omega_k & \frac{\tau_k}{\tau_Q} \end{pmatrix} \quad (62)$$

with $\tau_k = (\cos(k_1) + \cos(k_2) + t)$, $\Omega_k = |\sin k_1 - \sin k_2|$. Therefore, we need to know if $p_k(t)$ is quantitative, we need to look at two things: $\Omega_k \lesssim \tau_Q^{-\frac{1}{2}}$ and $\tau_k(t) > 0$. This can be resumed by one fact: at the k position, ε_k was small compared to $\tau_Q^{-\frac{1}{2}}$ at one point in its evolution. For instance, for $t < -2\tau_Q$, we are always in the gapped phase and therefore, there is no excitation. We will separate three situations: if we stop at the critical line ($t = -2\tau_Q$), if we stop inside the gapless phase ($-2\tau_Q < t < 0$), if we stop after the multicritical point ($t > 0$).

1. At the critical line

We stop first our evolution at the critical line i.e. $t = -2\tau_Q$. We have the spectrum represented in FIG. 6b: it is linear in one direction and quadratic in the other. Therefore, the region where the energy is small compared to $\tau_Q^{-\frac{1}{2}}$ is of size $\tau_Q^{-\frac{1}{2}}$ in the linear direction and $\tau_Q^{-\frac{1}{4}}$ in the other. In total, the area of this region where we have quantitative excitations is of size $\tau_Q^{-\frac{3}{4}}$, and it follows that the density of excitations scales as :

$$\nu \sim \tau_Q^{-\frac{3}{4}}. \quad (63)$$

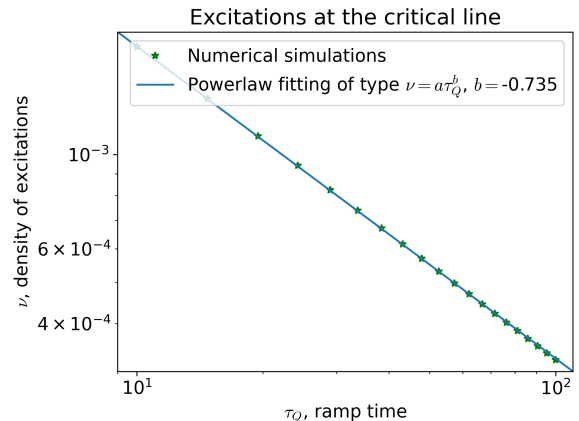


FIG. 9: Density of excitations after a ramp starting in the gapped phase and ending exactly at the phase transition. Theory predicts a density scaling as $\tau_Q^{-\frac{3}{4}}$, we do a power-law fit and it seems to follow this -0.75 factor.

This result is also found numerically, it is represented in FIG. 9.

This way of reasoning uses the same ideas as the Kibble-Zurek mechanism, but we have to adapt it a little because we have two directions with different z , this gives us a scaling of excitations:

$$\nu \sim \tau_Q^{-\frac{\nu z}{1+\nu z} \left(\frac{1}{z_x} + \frac{1}{z_y} \right)} \quad (64)$$

when we follow the same reasoning as in ID. This was in part done also by Hikichi and al. in [11], with a slightly different interpretation (but which comes to the same in the end).

2. In the gapless phase

Now we stop our evolution in the gapless phase, first, let's present the scaling of the excitations with Kibble-Zurek ideas. During the ramp, if we look at the spectrum we have this evolution: an anisotropic vanishing energy point appeared at $t = -2\tau_Q$, it then split into 2 Dirac cones with linear dispersion, these 2 Dirac cones then moved in the Brillouin zone. We have seen we have excitations in all the regions where the energy has been during the evolution smaller than $\tau_Q^{-\frac{1}{2}}$. Around a Dirac point, the energy has a linear dispersion, and therefore the region where there are excitations scales as $\tau_Q^{-\frac{1}{2}}$ in both directions (it is an area of size τ_Q^{-1}). However, during the evolution the Dirac cone moved in the Brillouin zone, the excitation was therefore integrated in

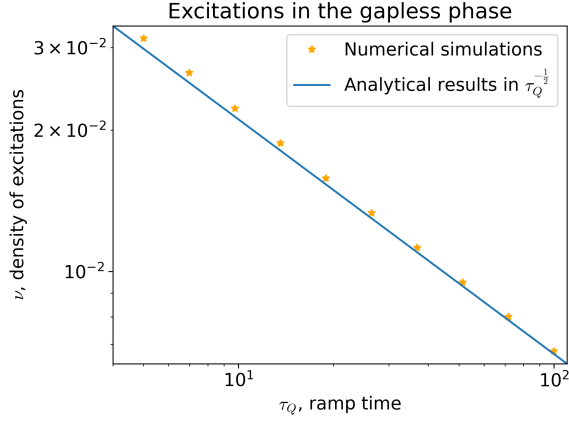


FIG. 10: Density of excitations after a ramp starting from the gapped phase and ending inside the gapless phase. The Kibble-Zurek mechanism predicts a $\tau_Q^{-\frac{1}{2}}$ scaling, we are here able to give an analytical result.

one direction where the extension of the region of excitations is of the order of 1. Thus, the scaling comes only from the orthogonal direction where we have $\tau_Q^{-\frac{1}{2}}$ scaling. Finally, we get a density of excitations :

$$\nu \sim \tau_Q^{-\frac{1}{2}} \quad (65)$$

This was a hand-waving argument but here in this solvable model, we can have an analytical result. As explained at the beginning of this subsection, we have for each k sector a Landau-Zener Hamiltonian given in (62). In particular, with the change of variable:

$$\begin{cases} \bar{k} = \frac{k_1 + k_2}{2} \\ \delta k = \frac{k_1 - k_2}{2} \end{cases} \quad (66)$$

we get

$$\begin{cases} \Omega_k = 2|\cos(\bar{k})\sin(\delta k)| \\ \tau_k = 2\tau_Q \cos(\bar{k})\cos(\delta k) + t \end{cases} \quad (67)$$

If we stop our evolution at $-2\tau_Q < t_f < 0$, we will get excitations for $|\delta k| \lesssim \tau_Q^{-\frac{1}{2}} \ll 1$ and for $|\bar{k}| < k_f = \arccos\left(\frac{t_f}{2\tau_Q}\right)$. In this region, we have the approximation

$$\Omega_k \simeq 2|\cos(\bar{k})||\delta k|. \quad (68)$$

With the expression of the Landau-Zener transition, we

finally get :

$$\nu = \int \frac{d^2k}{4\pi^2} P_k(t_f) \quad (69)$$

$$\simeq \frac{1}{2\pi^2} \int_{-k_f < \bar{k} < k_f} d\bar{k} \int_{\delta k} d\delta k \exp(-8\pi\tau_Q \cos(\bar{k})(\delta k)^2) \quad (70)$$

where the second integral spans over all the real axis because we can extend the integral where it is negligible. This gives us by integration :

$$\nu \simeq \frac{1}{\tau_Q^{\frac{1}{2}} 2\sqrt{2}\pi^2} \int_0^{k_f} \frac{d\bar{k}}{\cos(\bar{k})}. \quad (71)$$

We have here the scaling as $\tau_Q^{-\frac{1}{2}}$ with the exact prefactor (which can be expressed with trigonometric functions). We can also simulate this ramp numerically and we get the results in FIG. 10 for $t_f = -\tau_Q$. The analytical result fits the simulations for large values of τ_Q .

As a remark, this excitation is added to excitations we had on the critical line but the $\tau_Q^{-\frac{1}{2}}$ dominates the $\tau_Q^{-\frac{3}{4}}$ and therefore for large τ_Q we only see the excitations from the gapless phase evolution.

3. After the multicritical point

This subsection is new work that was not done previously. At the multicritical point, the spectrum behaves in a very peculiar fashion: it flattens in one direction on the line $\bar{k} = \pm\frac{\pi}{2}$ where the energy vanishes. To study it, we consider that we stop the study after going through all the ramp ($t_f = +\infty$), with this we have the excitation from the critical lines, the two gapless phases (which dominate the latter), and the multicritical point. We already know the excitations at the critical lines and in the gapless phases so we will be able to spot what happens at the multicritical point.

First, let's consider a scaling argument as before. At the multicritical point, we have a line where the energy vanishes and there is a linear dispersion in the other direction. Therefore, if we look at the region where the energy is smaller than $\tau_Q^{-\frac{1}{2}}$, it will be of scale as $\tau_Q^{-\frac{1}{2}}$.

In addition to the $\tau_Q^{-\frac{1}{2}}$ from the gapless phases, we get excitations as:

$$\nu \sim \tau_Q^{-\frac{1}{2}}. \quad (72)$$

We have done numerical simulations in FIG. 11, we multiplied the density of excitations by $\tau_Q^{\frac{1}{2}}$ but we do not get the constant line we expect from this computation.

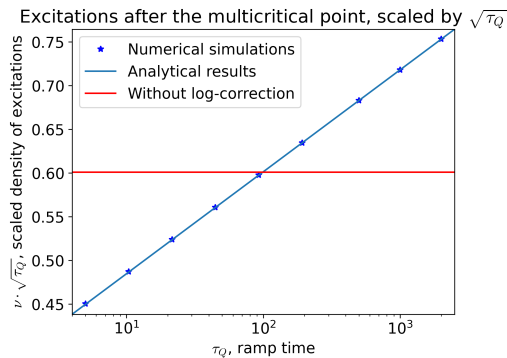


FIG. 11: Density of excitation after a ramp starting from the gapped phase, going through the two gapless phases and the multicritical point and ending in the gapped phase, multiplied by $\tau_Q^{\frac{1}{2}}$. The axes are semi-log and as the simulation points follow a nonconstant line, we have excitations as $\log(\tau_Q)\tau_Q^{-\frac{1}{2}}$.

This comes from the fact that just before becoming a vanishing line at the multicritical point, the Dirac cone was linear in both directions but almost zero in one direction. Thereby, there is more excitation than what we expected, let's dive into the computations to understand better.

This time as we ended the evolution at $t = +\infty$, all the Landau-Zener transitions were done and we only have to look at

$$\Omega_k = 2|\cos(\bar{k})\sin(\delta k)|. \quad (73)$$

We can consider the computation done in the last subsection, here we integrate over all the Brillouin all the Brillouin zone thus :

$$\nu \simeq \frac{1}{\tau_Q^{\frac{1}{2}}\sqrt{2}\pi^2} \int_0^{k_f} \frac{d\bar{k}}{\cos(\bar{k})} \quad (74)$$

with k_f going to $\frac{\pi}{2}$. However, this integral diverges because $\cos(x) \sim (x - \frac{\pi}{2})$ for $x \rightarrow \frac{\pi}{2}$. Therefore, the integral diverges as a log, but this comes from the fact that we did a too crude approximation near $\frac{\pi}{2}$, in practice, there will be a cutoff of size $\tau_Q^{-\frac{1}{2}}$ in this divergence and therefore we will have a scaling of the excitations as:

$$\nu \sim (a + b \log(\tau_Q)) \frac{1}{\sqrt{\tau_Q}} \quad (75)$$

with a and b some constants.

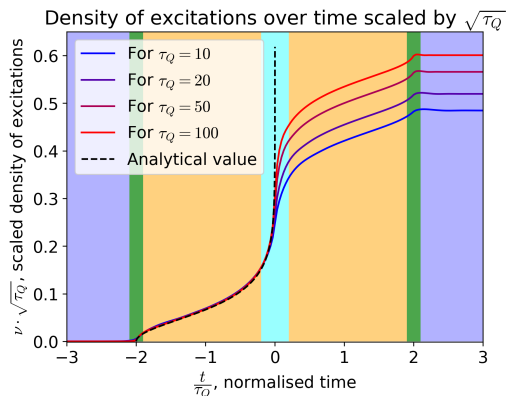


FIG. 12: Density of excitations over time in Kitaev model, multiplied by $\sqrt{\tau_Q}$. We have different scalings according to the phase in question. In particular, we have a perfect $\tau_Q^{-\frac{1}{2}}$ scaling in the gapless phase but at the critical point in addition to that, there is a $\log(\tau_Q)$ term.

For this ramp we can even compute explicitly the scaling (this is done in the appendix A) :

$$\nu = \frac{1}{\sqrt{2}\pi^2} \frac{1}{\sqrt{\tau_Q}} (\log(\tau_Q) + 4\log(2) + C) + O(\tau_Q^{-1}) \quad (76)$$

with $C \simeq 4.49453$ an integration constant. This scaling is observed in simulation as we can see in the FIG. 11 where we multiply by $\tau_Q^{\frac{1}{2}}$ and use semi-log axis to see the log-correction to the first idea of a $\tau_Q^{-\frac{1}{2}}$ scaling.

This log-correction seems to come from the fact that we are going through a phase transition between two gapless phases. We did not find another place where a similar log-correction was observed, in particular with no log in the dispersion, in the appendix B, I present some ideas of where a log-correction can come from.

As a conclusion of this part, we have FIG. 12 which represents the evolution of the density of excitations over time. We have different scaling of excitations depending on the moment but all the excitations are added to each other and in the end we get a $\log(\tau_Q)\tau_Q^{-\frac{1}{2}}$ scaling.

B. Periodic boundary condition on the extended model

In the extended model, we can do a similar ramp as in the original Kitaev model but this is not necessary. Here, we have only gapped phases and the spectrum is

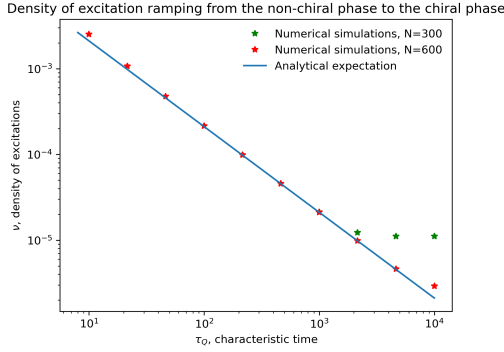


FIG. 13: Density of excitation going through the critical line. Here it means we are going from a non-chiral to a chiral phase. We have excitations going as τ_Q^{-1} , this is the Kibble-Zurek scaling. Here, we can see a good fit but finite size effect for large linear size N of the system.

gapless only at the phase transitions. Thus, the excitations only appear at the phase transition and we can look at them individually. Therefore we will do two ramps: $J_x = J_y = 1$ and $J_z = 2 \left(1 - \frac{t}{\tau_Q}\right)$ to study the critical line; and $J_x = J_y = 1$ and $J_z = -2 \frac{t}{\tau_Q}$ to study the multicritical point (each time we start before 0 and stop afterward).

Let's study the first ramp, here (and for the second ramp too), we are still in the same situation with a Hamiltonian in the form:

$$H(t) = \sum_k \chi_k^\dagger H_k(t) \chi_k \quad (77)$$

and the study is

$$\nu = \int \frac{d^2 k}{4\pi^2} p_k(t) \quad (78)$$

with $p_k(t)$ the probability of transition of $H_k(t)$. Now that we are going from gapped to gapped phase, at the phase transition, at $t = 0$, the spectrum has a vanishing gap at a linear Dirac cone. Therefore, the region where there is excitation i.e. where $\varepsilon_k \lesssim \tau_Q^{-\frac{1}{2}}$ is of size $\tau_Q^{-\frac{1}{2}}$ in both directions and therefore we have a scaling:

$$\nu \sim \tau_Q^{-1}. \quad (79)$$

This is the Kibble-Zurek scaling with $\nu = 1 = z$ and $d = 2$. Here, by looking at the explicit Landau-Zener

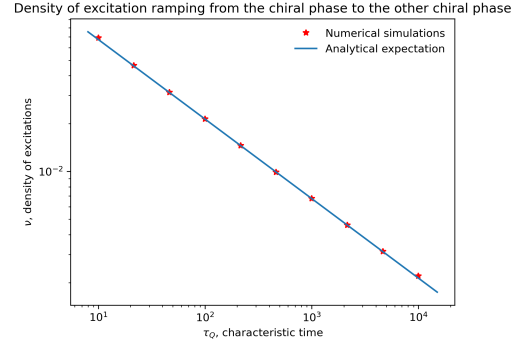


FIG. 14: Density of excitation after the multicritical point. Here it means we are going from one chiral phase to another. We see that the excitation follows the τ_Q^{-1} scaling.

transitions at each point (I do not present these computations), we can have an explicit value:

$$\nu \simeq \frac{1}{48\pi^2 \varepsilon} \frac{1}{\tau_Q}. \quad (80)$$

This is also what we get in numerical simulations as presented in FIG. 13.

If we now look at the second protocol, we are going from a chiral to the other chiral phase. At the phase transition, we still have the degeneracy of having a line where the energy is vanishing. However, in this evolution, it is the only thing happening and we do not have any log-correction. Therefore, we get the scaling

$$\nu \sim \tau_Q^{-\frac{1}{2}} \quad (81)$$

because it is the size of the region of linear dispersion around this line where the energy is below $\tau_Q^{-\frac{1}{2}}$. Here again, we can compute everything explicitly and we get:

$$\nu \simeq \frac{1}{\sqrt{\tau_Q}} \frac{1}{4\pi^2} I(\varepsilon) \quad (82)$$

with

$$I(\varepsilon) \stackrel{\varepsilon \rightarrow 0}{\simeq} 4 \log(\varepsilon) + C \quad (83)$$

with $C \simeq 1.62186$. In particular, we can interpret this equation as the fact that the log correction has been taken by the ε term which is the one giving the cutoff in the log divergence of the integral. We can see this in FIG. 14.

In the end, this extended model is easier than the original model because we do not have any gapless phase. However, it is still interesting because as we have a chiral phase we can also study the edge modes. But for that, we need to open the boundary by definition.

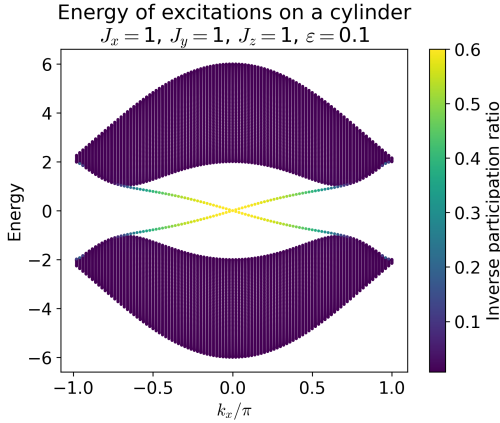


FIG. 15: Spectrum of the extended Kitaev model on a cylinder inside the chiral phase. We represent a dot for the energy of each eigenvector and choose the color to represent the inverse participation ratio. We see as expected in a chiral phase, the existence of edge states with an inverse participation ratio of the order of 1 and they live in the gap.

C. Excitation of the edge modes in the extended model

Here we study the ramp going from the non-chiral to the chiral phase, i.e. $J_x = J_y = 1$ and $J_z = 2 \left(1 - \frac{t}{\tau_Q}\right)$. We want to study the edge states so we need to open a boundary however it is also useful to have periodic boundary conditions in order to have conserved quantities. Thereby, we chose to put the system on a cylinder, that is, it is open in one direction (the y -direction in my study) and periodic in the other (the x -direction in my study).

Therefore, we can do a Fourier transform in the x direction and we get a Hamiltonian in the form:

$$H = \sum_{k_x} \chi_{k_x}^\dagger H_{k_x} \chi_{k_x} \quad (84)$$

with χ_{k_x} a N_y vector of annihilation operators for each ordinate y . We can do a Bogoliubov-De Gennes transformation with the eigenvectors $\psi_{k_x,i}(y)$ of H_{k_x} in order to get:

$$H = \sum_{k_x,i} \varepsilon_{k_x,i} \left(\gamma_{k_x,i}^\dagger \gamma_{k_x,i} - \frac{1}{2} \right). \quad (85)$$

If we consider a time-varying Hamiltonian, we have with

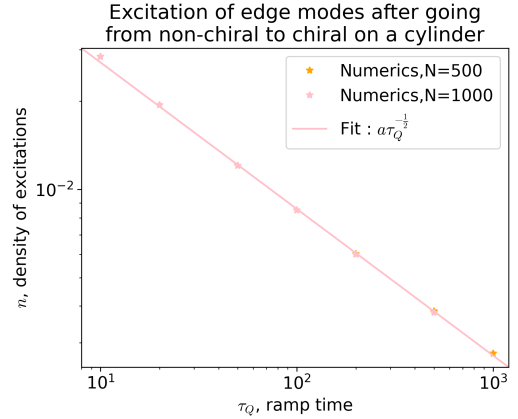


FIG. 16: Density of excitation of the edge modes in the extended model after going from the non-chiral to the chiral phase. We have a scaling as $\tau_Q^{-\frac{1}{2}}$, this is the Kibble-Zurek scaling for a dimension $d = 1$. There is little finite size effect for these sizes of systems (N is the linear size of the system: there are $2N^2$ sites).

the same reasoning as in the first section, that:

$$\nu = \frac{1}{N} \sum_{k_x,i} \left\langle \gamma_{g(t),k_x,i}^\dagger \gamma_{g(t),k_x,i} \right\rangle_t = \frac{1}{N} \sum_{k_x,i,j} p_{k_x,j \rightarrow i}(t) \quad (86)$$

with $p_{k_x,j \rightarrow i}(t)$ the probability of getting from the negative energy eigenstate i to the positive energy eigenstate j . In particular, we can spot the density of excitation of edge states by only summing the $p_{k_x,j \rightarrow i}$ for an edge state.

We therefore need a way to know whether a certain state is an edge state or not. For that, we can use the inverse participation ratio (IPR):

$$I_{k_x,i} = \sum_y |\psi_{k_x,i}(y)|^4. \quad (87)$$

This number is between 0 and 1 and if ψ is a wavefunction spanned uniformly over L sites then $I = \frac{1}{L}$. Therefore, in our system of size N_y for the eigenvectors, we have $I_{k_x,i}$ of the order of $\frac{1}{N_y}$ for the bulk modes but of the order of 1 for the edge modes. We can compute it for our system, one example is given in FIG. 15 with also a representation of the energy for each state. We see in particular that inside the chiral phase, we have edge states and they live in the gap. Now we can effectively choose the edge states as the states of inverse participation ratio greater than 0.2 (arbitrarily) and do the numerical simulation.

In the simulation of the evolution, we first notice that the edge states do not get excited inside the chiral phase even though they have vanishing energy: it may be because we do not have an evolution of the eigenstates and therefore there is no reason to be excited (they feel a constant Hamiltonian). However, we get excitation at the phase transition as presented in FIG. 16.

In this simulation, we spot that the density of excitations scales as $\tau_Q^{-\frac{1}{2}}$, this is the Kibble-Zurek excitation for this system ($\nu = z = 1$) with a dimension $d = 1$. This is logical because the edge modes live on the frontier which is of dimension 1.

CONCLUSION

In my work, I studied the Kitaev Honeycomb model and applied the Kibble-Zurek mechanism to get the scaling of the number of excitations after a ramp. The idea is to use these scalings to conceive an experimental protocol that creates only specific excitations: anyons. I did not have time to finish this part during my intern-

ship but I am still in discussion with my supervisors to do it.

Along the way, I encountered a logarithmic scaling that was not observed before in similar systems. It could be interesting to understand further what are the conditions that make it appear.

I would like to thank my supervisors Marin and Patrick who found me a really interesting project and prepared for me a lot of preliminary work such that I could be efficient upon my arrival at PKS. They were a lot helpful during my internship and afterward. I would also like to thank Michael and Tarik who helped make this project go further and gave a lot of ideas during our discussions. Moreover, I would like to thank all the students, researchers, and staff at PKS, they helped me a lot enjoy my stay at Dresden and have enriching conversations about physics. Finally, I would like to thank Nicolas, Sylvain, Matthieu, and of course Valens for their support and discussion during this internship.

-
- [1] M. Born and V. Fock, Beweis des adiabatsatzes, *Zeitschrift für Physik* **51**, 165 (1928).
- [2] C. Zener, Non-adiabatic crossing of energy levels, *Proceedings of the Royal Society of London. Series A, Containing Papers of a Mathematical and Physical Character* **137**, 696 (1932).
- [3] J. Dziarmaga, Dynamics of a quantum phase transition and relaxation to a steady state, *Advances in Physics* **59**, 1063 (2010).
- [4] T. W. Kibble, Topology of cosmic domains and strings, *Journal of Physics A: Mathematical and General* **9**, 1387 (1976).
- [5] W. H. Zurek, Cosmological experiments in superfluid helium?, *Nature* **317**, 505 (1985).
- [6] A. Kitaev, Anyons in an exactly solved model and beyond, *Annals of Physics* **321** (2006).
- [7] H.-D. Chen and Z. Nussinov, Exact results of the kitaev model on a hexagonal lattice: spin states, string and brane correlators, and anyonic excitations, *Journal of Physics A: Mathematical and Theoretical* **41**, 075001 (2008).
- [8] E. H. Lieb, Flux phase of the half-filled band, *Physical review letters* **73**, 2158 (1994).
- [9] B.-Y. Sun, N. Goldman, M. Aidelsburger, and M. Bukov, Engineering and probing non-abelian chiral spin liquids using periodically driven ultracold atoms, *PRX Quantum* **4**, 020329 (2023).
- [10] D. Das, S. R. Das, D. A. Galante, R. C. Myers, and K. Sengupta, An exactly solvable quench protocol for integrable spin models, *Journal of High Energy Physics* **2017**, 1 (2017).
- [11] T. Hikichi, S. Suzuki, and K. Sengupta, Slow quench dynamics of the kitaev model: Anisotropic critical point and effect of disorder, *Physical Review B—Condensed Matter and Materials Physics* **82**, 174305 (2010).
- [12] J. Dziarmaga, Dynamics of a quantum phase transition: Exact solution of the quantum ising model, *Physical review letters* **95**, 245701 (2005).

Appendix A: Computation of the log-correction

We want to study how many excitations are created from gapped to gapped when we go through the gapless phase and the multicritical point. This is given by :

$$\nu = \frac{1}{N} \sum_{k \in BZ} p_k \simeq \int_{k \in BZ} \frac{dk_1 dk_2}{4\pi^2} p_k \quad (\text{A1})$$

With p_k the Landau-Zener transition probability (at infinite time) of

$$H_k(t) = 2 \begin{pmatrix} -\frac{\tau_k}{\tau_Q} & \Omega_k \\ \Omega_k & \frac{\tau_k}{\tau_Q} \end{pmatrix} \quad (\text{A2})$$

with $\Omega_k = |\sin k_1 - \sin k_2|$. We therefore have :

$$p_k = e^{-\pi \tau_Q (\sin k_1 - \sin k_2)^2} \quad (\text{A3})$$

To study our problem, we take the change of variables of the average and the half-difference :

$$\begin{cases} \bar{k} = \frac{k_1 + k_2}{2} \\ \delta k = \frac{k_1 - k_2}{2} \end{cases} \quad (\text{A4})$$

We can spot that $k_x = \frac{2\sqrt{3}}{3}\bar{k}$ and $k_y = \frac{2}{3}\delta k$. In particular, the Brillouin zone won't have the same proportions as usual. The change of variable is of Jacobian $\frac{1}{2}$. Therefore, we can then rewrite :

$$\nu = \int_{k \in BZ} \frac{d\bar{k}d\delta k}{2\pi^2} \exp(-2\pi\tau_Q \sin^2(\delta k) \cos^2(\bar{k})) \quad (\text{A5})$$

We want the asymptotic value of ν when τ_Q is going to infinity. However, we have exponential decay of p_k when $|\sin(\delta k) \cos(\bar{k})| \lesssim \frac{1}{\sqrt{\tau_Q}}$. We have

$$\sin(\delta k) \cos(\bar{k}) = 0 \Leftrightarrow \delta k = 0 \text{ or } \bar{k} = \pm \frac{\pi}{2} \quad (\text{A6})$$

and we, therefore, study the neighborhood of this condition. We cut our Brillouin zone into 4 zones *A*, *B*, *C* and *D* as presented in Fig. 17. The idea is to be able to do different approximations depending on which region we are in. The cutoffs are such that $\bar{k}_{lim} = \pm \frac{\pi}{2} \pm \tau_Q^{-\frac{1}{6}}$ and $\delta k_{lim} = \pm \tau_Q^{-\frac{1}{6}}$. The choice of $\tau_Q^{-\frac{1}{6}}$ is arbitrary but the result does not depend on this choice of course. In general, to use the same approximations as we do, we could choose instead of $\frac{1}{6}$ some factor α such that $0 < \alpha < \frac{1}{4}$.

We have

$$\nu = \nu_A + \nu_B + \nu_C + \nu_D \quad (\text{A7})$$

such that

$$\nu_X = \int_{k \in X} \frac{d\bar{k}d\delta k}{2\pi^2} \exp(-2\pi\tau_Q \sin^2(\delta k) \cos^2(\bar{k})) \quad (\text{A8})$$

For $k \in A$, we have $|\delta k| \leq \tau_Q^{-\frac{1}{6}} \ll 1$. Therefore :

$$\nu_A \simeq 2 \int_{\substack{-\frac{\pi}{2} + \tau_Q^{-\frac{1}{6}} < \bar{k} < +\frac{\pi}{2} - \tau_Q^{-\frac{1}{6}} \\ -\tau_Q^{-\frac{1}{6}} < \delta k < \tau_Q^{-\frac{1}{6}}}} \frac{d\bar{k}d\delta k}{2\pi^2} \exp(-2\pi\tau_Q \delta k^2 \cos^2(\bar{k})) \quad (\text{A9})$$

Where the factor 2 comes from the fact that this is the integral of the central part of *A* which is half the total

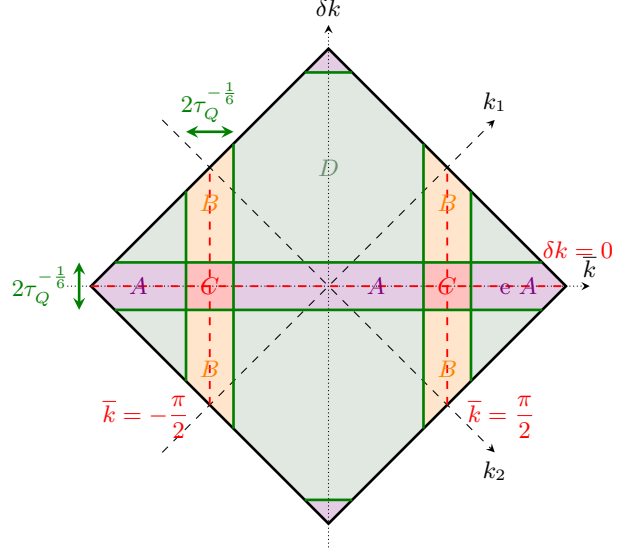


FIG. 17: Brillouin Zone separated into 4 regions

area. With the change of variable $u = 2\sqrt{\tau_Q}\delta k \cos(\bar{k})$, we get :

$$\nu_A = \frac{1}{\sqrt{2\pi^2}\sqrt{\tau_Q}} \int_{\substack{-\frac{\pi}{2} + \tau_Q^{-\frac{1}{6}} < \bar{k} < +\frac{\pi}{2} - \tau_Q^{-\frac{1}{6}} \\ -2\tau_Q^{\frac{1}{6}} \cos(\bar{k}) < u < 2\tau_Q^{\frac{1}{6}} \cos(\bar{k})}} \frac{d\bar{k}du}{\cos(\bar{k})} \exp(-\pi u^2) \quad (\text{A10})$$

In each of the Gaussian integrals, we have the limit at or above $2\tau_Q^{\frac{1}{6}} \cos\left(\frac{\pi}{2} - \tau_Q^{-\frac{1}{6}}\right) \simeq 2\tau_Q^{\frac{1}{6}} \gg 1$. Therefore, we can expand each of the Gaussian integrals to infinity and they are equal to 1. We get :

$$\nu_A \simeq \frac{1}{\sqrt{2\pi^2}\sqrt{\tau_Q}} \int_{-\frac{\pi}{2} + \tau_Q^{-\frac{1}{6}} < \bar{k} < +\frac{\pi}{2} - \tau_Q^{-\frac{1}{6}}} \frac{d\bar{k}}{\cos(\bar{k})} \quad (\text{A11})$$

The integrand is even, thus :

$$\nu_A \simeq \frac{\sqrt{2}}{\pi^2\sqrt{\tau_Q}} \int_{0 < \bar{k} < +\frac{\pi}{2} - \tau_Q^{-\frac{1}{6}}} \frac{d\bar{k}}{\cos(\bar{k})} \quad (\text{A12})$$

Here, we can understand why we get a logarithmic correction here: when $\bar{k} \rightarrow \frac{\pi}{2}$, $\cos(\bar{k}) \sim \left(\bar{k} - \frac{\pi}{2}\right)$ and therefore we integrate the function $x \mapsto \frac{1}{x}$. To have a better approximation, we use Wolfram|Alpha, to have :

$$\nu_A = \frac{\sqrt{2}}{\pi^2\sqrt{\tau_Q}} \left(-\log\left(\cos\left(\frac{\pi}{2}\right) - \sin\left(\frac{\pi}{2}\right)\right) + \log\left(\cos\left(\frac{\pi}{2}\right) + \sin\left(\frac{\pi}{2}\right)\right) \right) \quad (\text{A13})$$

With $x = \frac{\pi}{2} - \tau_Q^{-\frac{1}{6}}$. Therefore :

$$\nu_A \simeq \frac{\sqrt{2}}{6\pi^2} \frac{1}{\sqrt{\tau_Q}} \log(\tau_Q) + \frac{\sqrt{2}}{\pi^2} \frac{1}{\sqrt{\tau_Q}} \log(2) \quad (\text{A14})$$

We can see that if we exchange $\frac{\pi}{2} - \bar{k}$ and δk , we get the same computations between ν_A and ν_B . Therefore $\nu_A = \nu_B$. Moreover, in D , we have exponential decay of p_k , therefore $\nu_D \simeq 0$. We now have only to compute ν_C .

We consider the right part of C (the two parts have equal integral), therefore we have $|\delta k| < \tau_Q^{-\frac{1}{6}} \ll 1$ and $|\bar{k} - \frac{\pi}{2}| < \tau_Q^{-\frac{1}{6}} \ll 1$. We can then approximate p_k by :

$$p_k \simeq \exp\left(-2\pi\tau_Q(\delta k)^2\left(\bar{k} - \frac{\pi}{2}\right)^2\right) \quad (\text{A15})$$

By the change of variables $u_1 = \sqrt{2}\tau_Q^{\frac{1}{4}}\delta k$ and $u_2 = \sqrt{2}\tau_Q^{\frac{1}{4}}\left(\bar{k} - \frac{\pi}{2}\right)$, we get :

$$\nu_C = \frac{1}{\sqrt{2}\pi^2\sqrt{\tau_Q}} \int_{\left[-\sqrt{2}\tau_Q^{\frac{1}{2}}, \sqrt{2}\tau_Q^{\frac{1}{2}}\right]^2} du_1 du_2 \exp(-\pi u_1^2 u_2^2) \quad (\text{A16})$$

This is the integral of a function with the area growing with τ_Q . To get the scaling, we can consider only one side of the square, and in the neighborhood of the side, we have the integration of a Gaussian, which gives :

$$\nu_C = \frac{\sqrt{2}}{6\pi^2} \frac{1}{\sqrt{\tau_Q}} \log \tau_Q + O\left(\frac{1}{\sqrt{\tau_Q}}\right) \quad (\text{A17})$$

With Mathematica, we can numerically compute the $O\left(\frac{1}{\sqrt{\tau_Q}}\right)$, we get :

$$\nu_C = \frac{\sqrt{2}}{6\pi^2} \frac{1}{\sqrt{\tau_Q}} \log \tau_Q + \frac{1}{2\pi^2} \frac{1}{\sqrt{\tau_Q}} C \quad (\text{A18})$$

with $C \simeq 4.49453$.

This finally gives us :

$$\nu = \nu_A + \nu_B + \nu_C + \nu_D \quad (\text{A19})$$

$$= \frac{1}{\sqrt{2}\pi^2} \frac{1}{\sqrt{\tau_Q}} (\log(\tau_Q) + 4\log(2) + C) + O\left(\frac{1}{\tau_Q}\right) \quad (\text{A20})$$

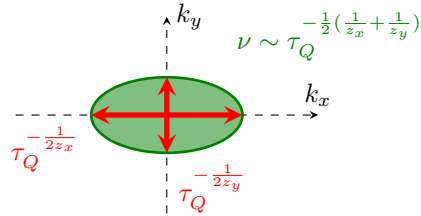
Which fits perfectly with the simulations, cf Fig. 11.

Appendix B: Circumstances of log-correction

The idea here is to understand when we can have a scaling with a log when studying the number of excitations of a system with out-of-equilibrium dynamics. We will first use some assumptions of a generic system. We consider having excitations labeled by a quasi-momentum k , with $k = (k_x, k_y)$. We suppose to have a time evolution of the energy $E(k, t)$ and we write $\Delta(k) = \min_t E(k, t)$. We will assume (it can be reasonable but I am not sure of when it is the case) that $\Delta(k)$ is in the form $|f(k)|$ with $f(k)$ an analytic function. We study the density of excitations represented by $\nu = \int \frac{dk_x dk_y}{4\pi^2} p_k$ the integral of the probability p_k of excitation of a particle of momentum k . If the evolution follows as precedently a Landau-Zener transition, $p_k = \exp(-\tau_Q \Delta(k)^2)$. This leads us to say that we have excitations if $\Delta(k) \lesssim \tau_Q^{-\frac{1}{2}}$. In general with an evolution ruled by the universality $E \sim (t/\tau_Q)^{\nu z}$, the adiabaticity is broken and therefore we have excitations when $\Delta(k) \lesssim \tau_Q^{-\frac{\nu z}{\nu z + 1}}$. I will continue with $\nu z = 1$ but it does not change the reasoning.

We now want to see the appearance of a log term when studying τ_Q going to $+\infty$.

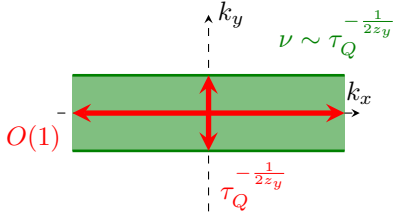
→ If $\Delta(k)$ is vanishing only at one point (wlog at $k = 0$) (it is the case for instance with a phase transition), then with a Taylor expansion we have $\Delta(k) \sim |k_x^{z_x} k_y^{z_y}|$. Therefore the region where $\Delta(k) \lesssim \tau_Q^{-1/2}$ is of the form as below :



We therefore have excitations scaling as $\tau_Q \tau_Q^{-\frac{1}{2}\left(\frac{1}{z_x} + \frac{1}{z_y}\right)}$ and no log-correction.

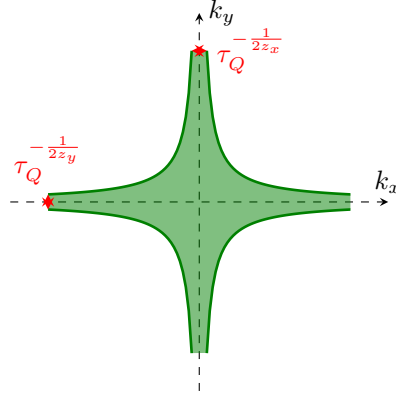
→ If $\Delta(k)$ is vanishing on a line (wlog at $k_x = 0$), it is the case when we are going through a gapless phase with a Dirac cone moving in the Brillouin zone or if we are going through a phase transition (between gapped phases) with a 1D degeneracy at the phase transition. Then with a Taylor expansion, we have $\Delta(k) \sim C k_y^{z_y}$ with C a constant (in general it could depend on k_x but it doesn't change the scaling). Therefore the region

where $\Delta(k) \lesssim \tau_Q^{-1/2}$ is of the form as below :



We therefore have excitations scaling as $\tau_Q^{-\frac{1}{2z_y}}$ and no log-correction.

→ The interesting case is when we have two intersecting lines where $\Delta(k)$ is vanishing (wlog on $k_x = 0$ and $k_y = 0$). It can happen when we are going from a gapless phase to a gapless phase with a 1D degeneracy at the phase transition, I think it could also happen if two Dirac cones merge at a phase transition and then separate again. With a Taylor expansion, we have $\Delta(k_x \simeq 0, k_y) \simeq C(k_y) \cdot k_x^{z_x}$ and $\Delta(k_x, k_y \simeq 0) \simeq D(k_x) \cdot k_y^{z_y}$ with $C(k_y)$ and $D(k_x)$ non vanishing constants (for $k_x \neq 0$ and $k_y \neq 0$). This gives/comes from $\partial_x^\alpha \Delta(0, k_y) = 0$ for $\alpha < z_x$ and $\partial_y^\beta \Delta(k_x, 0) = 0$ for $\beta < z_y$. Consequently, $\partial_x^\alpha \partial_y^\beta \Delta(0, 0) = 0$ for $\alpha < z_x$ or $\beta < z_y$. By Taylor expansion, the first non-vanishing term is : $\Delta(k_x \simeq 0, k_y \simeq 0) \simeq \lambda k_x^{z_x} k_y^{z_y}$ with λ a non vanishing constant. This gives us the region where $\Delta(k) \lesssim \tau_Q^{-1/2}$ is of the form as below :



If we are near the $k_x = 0$ axis but far from the $k_y = 0$ then the excitations scale as $\tau_Q^{-\frac{1}{2z_y}}$ and for the other axis it is as $\tau_Q^{-\frac{1}{2z_x}}$. However, for the central region, it depends on z_x and z_y . On one hand, if z_x and z_y are different they are dominated by the larger of the smaller of the two, and if for instance $z_x < z_y$ then the excitations scales as $\tau_Q^{-\frac{1}{z_x}}$ and in total $\nu \sim \tau_Q^{-\frac{1}{z_x}}$. But on the other hand, if $z_x = z_y$, then the central area is a hyperbola and the excitations scale as $\tau_Q^{-\frac{1}{z_x}} \log(\tau_Q)$. In total we therefore have excitations :

$$\nu \sim \tau_Q^{-\frac{1}{z_x}} \log(\tau_Q)$$

In conclusion, we seem to have a log correction when we are specifically going from a gapless phase to a gapless phase but we also need another characteristic given by $z_x = z_y$ which is true for the Kitaev case where $z_x = z_y = 1$.